

PRELIMINARY RESULTS ON XENOLITHS IN BASALTIC ANDESITE SUBVOLCANIC BODY IN THE VICINITY OF KROUMOVGRAD, EASTERN RHODOPES, BULGARIA

Nedialkov R.

*Department of Mineralogy, Petrology and Economic Geology, Faculty of Geology and Geography,
Sofia University "St. Kliment Ohridski", rmed@gea.uni-sofia.bg*

Abstract: The studied basaltic andesite subvolcanic body belongs to the Paleogene post-collisional volcanism of the Eastern Rhodopes Momchilgrad-Arda volcanic region. It intrudes acid and intermediate pyroclastic, epiclastic rocks as well as concomitant sedimentary rocks. The subvolcanic rocks are with dense porphyritic texture and glassy (hyalinic) ground mass. Phenocrysts are represented by clinopyroxene, orthopyroxene and plagioclase. The rocks are medium-K to high-K, Q-normative and with $Mg\# = 65-72$. Their geochemical peculiarities are similar to those from subduction related magmas, with negative anomalies for Ta, Nb, Ti, P in primordial mantle normalized spidergrams, but are probably influenced by lower crust material. Three different types of deep xenoliths of granulites, plagioclasites and cumulate clinopyroxenites are established. Granulites are metabasites with $MgO = 7.15$ wt. %. Basic granulites (pyriclasites) are composed by clinopyroxene and plagioclase where titanomagnetite is an accessory phase. Plagioclasites are composed exclusively of oligoclase with a small amount of chlorite. And finally clinopyroxenites are monomineral but with a transitional peripheral zone, where plagioclase (anorthite) appears as a reaction product. Pressure estimations for granulites and clinopyroxenites are 8-14 kbars corresponding approximately to the crust – mantle boundary. Both xenolith types show petrographic evidences for rock transformations and initial melting. They were probably the result of an interaction with the ascending-basaltic to basaltic andesite mantle-derived and lower crust modified magma.

Keywords: East Rhodopes, Paleogene volcanism, subvolcanic basaltic andesites, deep coming xenoliths.

1. Introduction

The calc-alkaline to shoshonitic volcanic activity in the Eastern Rhodopes is collision-related (Yanev et al., 1989) or post-collisional (Ivanov, 1988) with Paleogene age (Priabonian and mainly Oligocene) (Lilov et al., 1987; Harkovska et al., 1989). The investigations on the Paleogene volcanism, based on precise geochemistry and isotopic analyses, have revealed that the magmatic source is enriched metasomatised mantle (Marchev et al., 1989, 1994; Nedialkov and Pe-Piper, 1998; Yanev, 2003), and that derived melts have been crustal contaminated. The investigations on coeval alkaline basaltic dikes of intraplate origin, disposed 20-30 km southeast from the town of Kroumovgrad, presented evidence for the role of the underplating of basaltic magma for the core complex formation and first data about the composition of the most upper parts of the lithospheric mantle as well as the transition to the lower crust in the Eastern Rhodopes (Marchev et al., 2006). Deep derived xen-

liths were not established until now in the collision related volcanites. The recently discovered xenoliths of pyroxenites, eclogites and plagioclasites in a basaltic andesite subvolcanic body, western of Kroumovgrad, present the possibility to obtain new information for the upper mantle – lower crust transition in the region and to examine some elements (characters) of the interaction between the melt and deep seated rocks.

2. Geological setting

In the Eastern Rhodopes the Paleogene volcanism is emplaced in two structural depressions: the Borovitsa volcanic region, situated in the North, and the Momchilgrade-Arda volcanic region (MAVR), being to the south. Several subvolcanic, basaltic andesite to shoshonite bodies are disposed at the south-eastern border of MAVR at the vicinities of the town of Kroumovgrad (Gorna Koula, Vransko, Loulichka, and Akpoba Kajasi). The subvolcanic

body near the village of Gorna Koula represents a spectacular outcrop, disposed in a small river valley at 1.5 km westward of the Kroumovitza River and the town of Kroumovgrad.

The subvolcanic body intrudes first acid volcanism pyroclastic deposits (fall and flow) as well as pyroclastic and epiclastic ones with intermediate composition (Moskovski et al., 1996; Fig. 1) from the second intermediate volcanism (Ivanov, 1960). The acid pyroclastics are represented by agglomerate breccia, lapilli and coarse ash tuffs of white, pale greenish and pale yellow color deposited in a shallow marine basin. They associate with tuffaceous siltstones and marls, conglomerates and sandstones. The rocks of intermediate composition are represented by andesitic tuffs, tuffites, breccias as well as black silicic mudstones and organogenic reef limestones. The host pyroclastic rocks were water-rich and not well (solidified) lithified at the moment of the subvolcanic intrusion. The subvolcanic body is sill-like or lens-like, subhorizontal, with meridional length of approximately 1 km, width of up to 250 m and height of about 50-60 m. It has complicated internal concentric structure resulting from two stage (2 impulses) magma injection. The concentric zones have radial columnar texture. The contacts with the host tuffs are sharp, in places – curvilinear and with small apophyses at the upper contact. Tuffs are silicified near the contact.

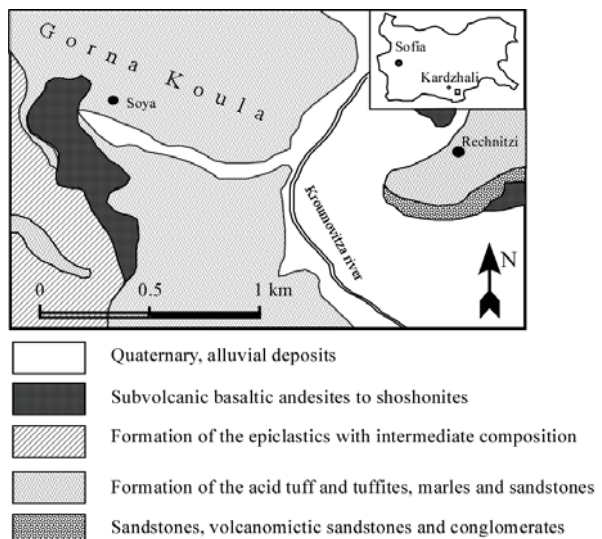


Fig. 1. Geological schematic map of the area of the subvolcanic body (after Moskovski et al., 1996, simplified).

3. Methods

Whole rock major element analyses were deter-

mined by a wet chemical method at the faculty of Geology and Geography of the Sofia University “St. Kl. Ohrodski”. For the basaltic andesites, trace elements Ba, Rb, Sr, Y, Zr, Nb, Pb, Ga, Zn, Cu, Ni, V and Cr were determined from pressed powder pellets on a Phillips PW 1400 sequential X-ray fluorescence spectrometer, using Rd-anode X-ray tube and the REE and Hf, Ta, Th, U, Sc and Sc by instrumental neutron activation analysis, at the Regional Geochemical Center, Department of Geology, St. Mary’s University, Halifax, N.S., Canada. Trace elements Cr, Ni, Cu, Zn, Rb, Ba for the granulite, and Co and Li for all the samples were analyzed with atomic absorption analysis at the Sofia University. Mineral chemistry was determined by electron microprobe – JEOL – 733 Superprobe – EDS at 15 or 25 Kev and accelerating potential for 100 seconds at EUROTTEST-CONTROL P/c, Sofia.

4. Results

4.1. Petrography

The basaltic andesite has dense porphyritic texture (phenocrysts up to 55-75% of the rock) and glassy groundmass near the contact. The internal parts of the body are almost holocrystalline with less than 20% recrystallized glassy ground mass. In some places the body is represented by holocrystalline gabbro where cracks with chilled melt (brownish volcanic glass) are observed. Two types of volcanic glass (brownish and pale rose), including skeletal plagioclases and ore minerals are established in the groundmass close to the contact (Fig. 2). Basaltic andesite's mineral composition is plagioclase (70-75 %), clinopyroxene (12-18 %), orthopyroxene (5 %) and titanomagnetite (2-3 %). Plagioclases have inverted zonal arrangement (bituminous core – An₈₀, labradorite-andesine intermediate zones – An₄₀₋₅₅ and bituminous rime – An₈₁). The clinopyroxene is augite (En₄₁₋₄₄, Fs₁₂₋₁₉, Wo₃₈₋₄₄, Ac₀₋₃). Orthopyroxene is enstatite (Fs₂₈₋₃₁). Accessory minerals are titanomagnetite (TiO₂ – 10-14 wt. %) and apatite.

In the subvolcanic body different types of xenoliths are found: clinopyroxenites, clinopyroxene granulites and plagioclases (oligoclasites) (Fig. 3). Clinopyroxenite is dark green-grey in color, medium grained, equigranular, composed entirely of pale green colored diopside (En₂₉₋₃₁, Fs₂₀, Wo₄₉₋₅₁; Tab. 1), with slight pleochroism and showing clearly higher content of alumina than the basaltic andesite clinopyroxenes (Fig. 4). Around the xenolith is observed a transitional reaction zone

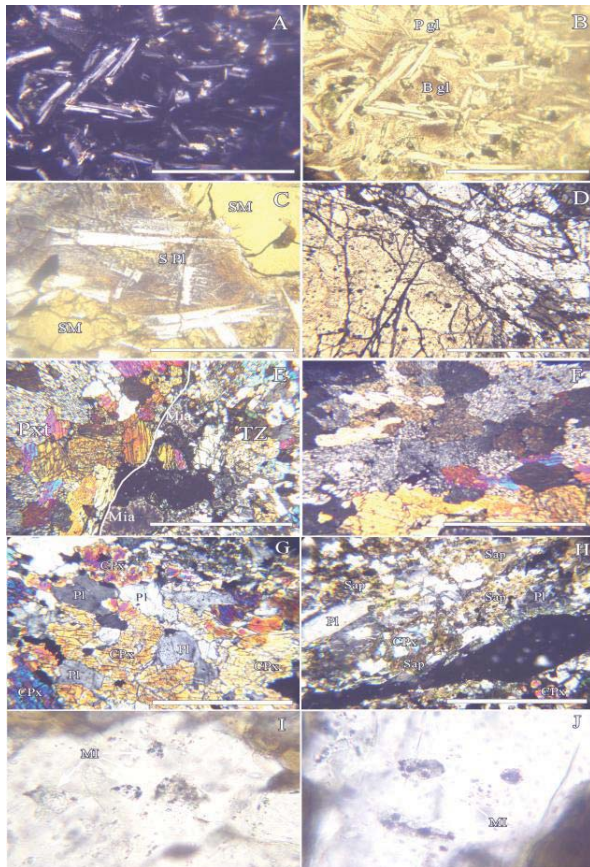


Fig. 2. Petrographic peculiarities of the studied rocks: A and B – groundmass of the basaltic andesite with miacoliths of plagioclase and two volcanic glasses: brown glass (B gl) relatively more basic ($\text{SiO}_2 = 62\text{-}64 \text{ wt. \%}$) and pale rose glass (P gl) with acid composition ($\text{SiO}_2 = 72 \text{ wt. \%}$); A – crossed Nikols; B – parallel Nikols; scale bar = 100 μm . C – skeletal plagioclase microliths (S Pl) in volcanic glass. SM – miacoles with secondary minerals (cryptocrystalline saponite and chlorite/smectite (?)); II N, scale bar = 100 μm . D - Plagioclase with oligoclase composition despite the different grain dimensions: II N, scale bar = 1 mm. E – Clinopyroxenite xenolith (Pxt), fine- to medium grained with equigranular, paneuhedral texture, composed entirely of clinopyroxene and the transitional zone of the xenolith (TZ) composed of clinopyroxene with small plagioclase inclusions, plagioclase grains and miacoles (Mia) filled with secondary minerals, marking the beginning of the transitional zone; the white line show the border between the Clinopyroxenite and the transitional zone; X N, scale bar = 2 mm. F – Clinopyroxenite; X N, scale bar = 2 mm. G – finegrained equigranular, granoblastic texture of a clinopyroxene basic granulite; Pl – plagioclase; Cpx – clinopyroxene; X N, scale bar = 0.6 mm. H – retromorphosed granulite with saponite (Sap) replacing mainly pyroxenes and occasionally plagioclase; X N, scale bar = 0.6 mm. I and J – mineral-melt inclusions in plagioclases from granulites; MI – mineral-melt inclusions with small fluid bubble and different small minerals (apatite, ore minerals and other undefined phases); II N, scale bar = 60 μm .

(2-5 mm thickness; Fig. 2 and 3). Plagioclase mineral inclusions (An_{93-99}) are found in clinopyroxenes (plagioclase nucleation on the expense of clinopyroxene) as well as small individual plagioclase grains, the composition of which gradually decreases in anortitic component toward the hosting basaltic andesite (Tab. 2). Small miacoles (up to 1.5mm) fulfilled with secondary minerals (chalcedony) are also observed in the transitional zone.



Fig. 3. Xenoliths and miacoles in the subvolcanic basaltic andesites. A – xenolith of plagioclase. B – xenolith of a clinopyroxenite: 1 – host basaltic andesite; 2 – transition zone between the host rock and the clinopyroxenitic xenolith; 3 – clinopyroxenitic xenolith; scale bar = 1 cm. C – miacoles filed with chalcedony (agate).

The clinopyroxene basic granulite (pyrclasites after Fettes and Desmons, 2007) is fine- to medium-grained and has a granoblastic texture (Fig. 2G). Plagioclase is andesine to labradorite (An_{44-55}). Clinopyroxene is augite (En_{37-45} , Fs_{14-18} , Wo_{37-38} , Ac_{0-5} ; Tab. 1). Accessory minerals are titanomagnetite ($\text{TiO}_2 = 35\text{-}37 \text{ wt. \%}$) and rare small apatite. The granulite is a metabasite with $\text{SiO}_2 = 47 \text{ wt. \%}$ and $\text{MgO} = 7.15 \text{ wt. \%}$ (Tab. 3). In plagioclases can be found numerous melt inclusions similar to those observed in plagioclases from volcanic rocks (Fig. 2I and J). Melt-inclusions have round or irregular shape, with dimensions of up to 35 μm , oc-

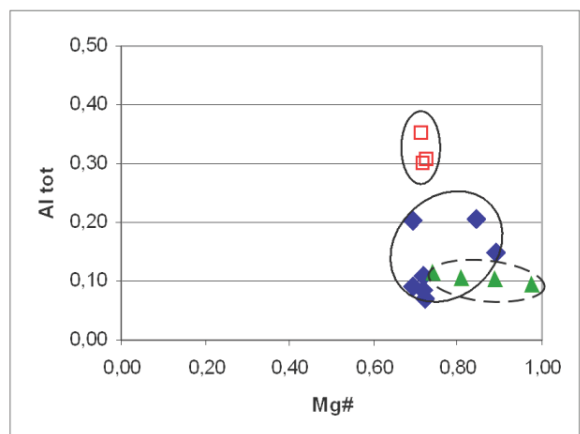


Fig. 4. Al_{tot} – $\text{Mg}\#$ diagram for the composition of clinopyroxenes from the host basaltic andesite (\blacklozenge) and from the clinopyroxenite (\square) and granulite (\blacktriangle) xenoliths.

Table 1. Chemical composition (in wt %) and structural formulae (on 6 O) of pyroxenes from subvolcanic basaltic andesites and clinopyroxenitic xenolith.

| Sample | 013kc3 | 1216 | 3195 | 013kc3 | 013kc3 | 013kc3 | 1216 | 3195 | 013kc3 | 013kc3 | 013kc3 | 013kc3 | 1216x2 | 1216x2 | 1216x2 | | |
|--------------------------------|-------------|-------------|-------------|-------------|-------------|-------------|-------------|-------------|-------------|-------------|-------------|-------------|-------------|-------------|-------------|-------------|-------------|
| Rock | BA | PXT | PXT | PXT | PXT | PXT | granulite | granulite | granulite | | |
| Location | CPx | CPx | CPx | CPx | CPx | Opx | Opx | CPx | | |
| SiO ₂ | 49,46 | 51,18 | 51,92 | 53,57 | 49,31 | 49,34 | 52,68 | 52,77 | 46,12 | 46,62 | 46,61 | 52,09 | 50,47 | 51,38 | 52,52 | 51,67 | 52,49 |
| TiO ₂ | 0,58 | 0,62 | 0,23 | 0,39 | 0,33 | 0,53 | 0,84 | 0,19 | 0,51 | 0,44 | 0,54 | 0,23 | 0,47 | 0,27 | 0,3 | 0,25 | 0,6 |
| Al ₂ O ₃ | 4,66 | 2,46 | 3,38 | 1,96 | 4,55 | 3,69 | 2,13 | 1,63 | 7,82 | 6,65 | 6,8 | 4,13 | 5,31 | 2,2 | 2,34 | 2,15 | 2,43 |
| FeO | 8,46 | 11,89 | 7,11 | 10,14 | 10,88 | 11,65 | 18,8 | 18,98 | 12,27 | 12,62 | 12,06 | 8,66 | 7,69 | 8,96 | 8,99 | 9,59 | 10,69 |
| MnO | 0,27 | 0,03 | 0,32 | 0,32 | 0,11 | 0,24 | 0 | 0,29 | 0,1 | 0,11 | 0,17 | 0 | 0 | 0,12 | 0,18 | 0,15 | 0,19 |
| MgO | 15,59 | 15,46 | 16,16 | 14,66 | 11,92 | 15,05 | 23,63 | 23,59 | 9,79 | 10,12 | 10,52 | 13,11 | 14,39 | 15,96 | 15,9 | 16,25 | 15,61 |
| CaO | 20,6 | 18,23 | 19,78 | 18,83 | 22,25 | 17,89 | 2,06 | 1,81 | 24,15 | 24,02 | 23,54 | 21,7 | 21,66 | 19,16 | 18,44 | 19,1 | 18,01 |
| Na ₂ O | 0 | 0 | 0,92 | 0 | 0 | 1,19 | 0,05 | 0,49 | 0 | 0 | 0 | 0 | 0 | 0,99 | 0,76 | 1,52 | 0 |
| K ₂ O | 0 | 0 | 0 | 0 | 0 | 0 | 0,07 | 0 | 0 | 0 | 0 | 0 | 0,05 | 0 | 0,09 | 0,04 | 0 |
| Total | 99,66 | 99,95 | 99,86 | 99,9 | 99,39 | 99,58 | 100,2 | 99,77 | 100,79 | 100,61 | 100,26 | 99,93 | 100,7 | 99,04 | 99,52 | 100,72 | 100,02 |
| Si | 1,85 | 1,92 | 1,92 | 1,98 | 1,87 | 1,87 | 1,93 | 1,95 | 1,76 | 1,78 | 1,78 | 1,93 | 1,87 | 1,93 | 1,95 | 1,92 | 1,95 |
| Al ^{IV} | 0,15 | 0,08 | 0,08 | 0,02 | 0,13 | 0,13 | 0,07 | 0,05 | 0,24 | 0,22 | 0,22 | 0,07 | 0,13 | 0,07 | 0,05 | 0,08 | 0,05 |
| Al ^{VI} | 0,05 | 0,03 | 0,06 | 0,07 | 0,08 | 0,03 | 0,02 | 0,02 | 0,11 | 0,08 | 0,09 | 0,11 | 0,10 | 0,02 | 0,05 | 0,01 | 0,05 |
| Fe ³⁺ | 0,10 | 0,03 | 0,11 | 0,00 | 0,05 | 0,24 | 0,01 | 0,08 | 0,16 | 0,17 | 0,16 | 0,00 | 0,01 | 0,15 | 0,06 | 0,25 | 0,00 |
| Ti | 0,02 | 0,02 | 0,01 | 0,01 | 0,01 | 0,02 | 0,02 | 0,01 | 0,01 | 0,01 | 0,02 | 0,01 | 0,01 | 0,01 | 0,01 | 0,01 | 0,02 |
| Fe ²⁺ | 0,16 | 0,34 | 0,11 | 0,32 | 0,30 | 0,12 | 0,57 | 0,50 | 0,22 | 0,23 | 0,22 | 0,27 | 0,22 | 0,12 | 0,22 | 0,04 | 0,33 |
| Mn | 0,01 | 0,00 | 0,01 | 0,01 | 0,00 | 0,01 | 0,00 | 0,01 | 0,00 | 0,00 | 0,01 | 0,00 | 0,00 | 0,01 | 0,00 | 0,01 | 0,01 |
| Mg | 0,87 | 0,86 | 0,89 | 0,81 | 0,68 | 0,85 | 1,29 | 1,30 | 0,56 | 0,58 | 0,60 | 0,72 | 0,79 | 0,89 | 0,88 | 0,90 | 0,86 |
| Ca | 0,82 | 0,73 | 0,78 | 0,75 | 0,91 | 0,72 | 0,08 | 0,07 | 0,98 | 0,98 | 0,96 | 0,86 | 0,86 | 0,77 | 0,73 | 0,76 | 0,72 |
| Na | 0,00 | 0,00 | 0,07 | 0,00 | 0,00 | 0,09 | 0,00 | 0,04 | 0,00 | 0,00 | 0,00 | 0,00 | 0,00 | 0,07 | 0,05 | 0,11 | 0,00 |
| K | 0,00 | 0,00 | 0,00 | 0,00 | 0,00 | 0,00 | 0,00 | 0,00 | 0,00 | 0,00 | 0,00 | 0,00 | 0,00 | 0,00 | 0,00 | 0,00 | 0,00 |
| Mg# | 0,84 | 0,72 | 0,89 | 0,72 | 0,69 | 0,87 | 0,69 | 0,72 | 0,71 | 0,72 | 0,73 | 0,73 | 0,78 | 0,88 | 0,80 | 0,96 | 0,72 |
| Wo | 41,99 | 37,19 | 39,81 | 39,66 | 46,96 | 35,72 | 4,15 | 3,59 | 51,06 | 50,15 | 49,45 | 46,42 | 45,43 | 38,20 | 37,58 | 36,79 | 37,32 |
| En | 44,22 | 43,89 | 45,26 | 42,97 | 35,01 | 41,81 | 66,17 | 65,05 | 28,80 | 29,40 | 30,75 | 39,02 | 42,00 | 44,28 | 45,09 | 43,56 | 45,01 |
| Fs | 13,78 | 18,93 | 11,58 | 17,36 | 18,04 | 18,17 | 29,51 | 29,61 | 20,14 | 20,45 | 19,80 | 14,56 | 12,57 | 13,95 | 14,52 | 14,34 | 17,67 |
| Ac | 0,00 | 0,00 | 3,35 | 0,00 | 0,00 | 4,30 | 0,18 | 1,76 | 0,00 | 0,00 | 0,00 | 0,00 | 0,00 | 3,57 | 2,80 | 5,30 | 0,00 |

BA - basaltic andesite; PXT - clinopyroxenite; CPx - clinopyroxene; Opx - orthopyroxene

curring in patches grouping 3 to 8 inclusions. They represent chilled melt, comprising one or more bubbles, and several very small different minerals (apatite, ore minerals and other undetermined phases). Granulites have undergone a partial retrogression (low temperature hydrothermal alteration) with an occasional replacement of the pyroxenes and plagioclases by saponite, oriented with conformity to the schistosity (Fig. 2H).

Plagioclases are found as angular brightly colored xenoliths with dimensions up to 25 cm. They are coarse grained (up to 5 mm), with brecciated and recrystallized finegrained zones. They are composed almost solely by oligoclase (An_{19-20} , Or_7 ; Tab. 3) and occasionally include small amounts of pale and brownish chlorite.

4.2. Geochemistry

Subvolcanic basaltic andesites to shoshonites (Fig. 5) are calc-alkaline to high-K calc-alkaline rocks, with relatively high potassium contents (medium-to high-K; Fig. 5B), with $Mg\# = 62-75$ and all samples are Q-normative. Primitive mantle normalized spidergrams (Sun and McDonough, 1989; Fig. 6) show negative anomalies for Ta, Nb, P and

Ti, typical for subduction related magmas. Chondrite-normalized REE patterns (Fig. 7) show enrichment in LREE ($La/Yb = 6.5 - 9$) and a small Eu anomaly ($Eu/Eu^* = 0.84-0.94$). The studied rocks plot close to the amphibolite fusion trend on the Ce_n/Yb_n-Ce_n diagram (after Gill, 1981; Fig. 8).

The temperature estimations for pyroxenites, based on pyroxene geothermometer (Weels 1977), show crystallizing temperatures of 1085–1095 °C. Temperatures for the basaltic andesites are 1120–1190°C. Pressure estimations we have made, based on clinopyroxenes (Nimis, 1999; Putirka, 2008) for granulites and pyroxenites, give very scattered unrealistic results. The clinopyroxene's compositions from the pyroxenite xenolith are very similar to those determined by Marchev et al. (2006) for pyroxenite xenoliths from the alkaline basaltic and lamprophyric dikes southeastern of Kroumovgrad. They have estimated pressures of crystallization to 7.5–13 kilobars (depth – 22–38 km), which is characteristic for the lower crust or the boundary lower crust – lithospheric mantle. Geophysical investigations have determined the Moho boundary in the Eastern Rhodopes at a depth of 32–38 km (Velchev et al., 1971; Yossifov and Pčelarov, 1977).

Table 2. Chemical composition (in wt. %) and structural formulae (based on 8 O) of plagioclases from basaltic andesite and xenolithes.

| Sample | 013kc3 | 013kc3 | 3175 | 013kc3 | 013x3 | 013x3 | 013x3 | 013x3 | 013kc1 | 013kc1 | 1216x2 | 1216x2 | 1216x2 | 1216x2 |
|--------------------------------|--------|--------|--------|-----------|-------|-------|-------|--------|----------|--------|-----------|-----------|-----------|-----------|
| Rock | BA | BA | BA | PXT | PXT | PXT | PXT | PXT | Plt | Plt | granulite | granulite | granulite | granulite |
| Location | Pl | Pl | Pl | Pl in CPx | Pl | Pl | Pl | Pl | Pl small | Pl | Pl | Pl | Pl | Pl |
| SiO ₂ | 47,37 | 52,67 | 49,75 | 44,21 | 48,79 | 46,92 | 51,75 | 54,29 | 59,97 | 62,9 | 52,16 | 55,17 | 57,88 | 54,07 |
| Al ₂ O ₃ | 32,96 | 27,99 | 31,26 | 35,65 | 31,98 | 33,23 | 28,15 | 28,13 | 24,17 | 22,34 | 25,69 | 26,96 | 25,09 | 27,48 |
| FeO | 0,81 | 1,10 | 0,84 | 0,92 | 1,09 | 0,68 | 0,86 | 0,85 | 0,08 | 0 | 2,38 | 0,66 | 0,42 | 0,43 |
| CaO | 16,41 | 10,83 | 13,68 | 17,96 | 16,58 | 17,04 | 12,77 | 12,33 | 4,59 | 4,71 | 10,64 | 11,83 | 9,53 | 11,37 |
| Na ₂ O | 1,94 | 5,89 | 4,13 | 0,74 | 1,17 | 1,15 | 4,47 | 4,61 | 9,77 | 8,16 | 6,5 | 5,1 | 6,29 | 5,85 |
| K ₂ O | 0,14 | 0,54 | 0,34 | 0 | 0,23 | 0,07 | 0,32 | 0,38 | 1,39 | 1,44 | 0,36 | 0,32 | 0,54 | 0,4 |
| Total | 99,65 | 99,02 | 100,03 | 99,52 | 99,93 | 99,1 | 98,32 | 100,71 | 100 | 99,58 | 99,14 | 100,38 | 99,77 | 99,62 |
| Si | 2,19 | 2,43 | 2,28 | 2,05 | 2,24 | 2,18 | 2,40 | 2,45 | 2,70 | 2,81 | 2,46 | 2,50 | 2,61 | 2,47 |
| Al | 1,79 | 1,52 | 1,69 | 1,95 | 1,73 | 1,82 | 1,54 | 1,50 | 1,28 | 1,18 | 1,43 | 1,44 | 1,34 | 1,48 |
| Fe(ii) | 0,03 | 0,04 | 0,03 | 0,04 | 0,04 | 0,03 | 0,03 | 0,03 | 0,00 | 0,00 | 0,09 | 0,03 | 0,02 | 0,02 |
| Ca | 0,81 | 0,54 | 0,67 | 0,89 | 0,82 | 0,85 | 0,64 | 0,60 | 0,22 | 0,23 | 0,54 | 0,57 | 0,46 | 0,56 |
| Na | 0,17 | 0,53 | 0,37 | 0,07 | 0,10 | 0,10 | 0,40 | 0,40 | 0,85 | 0,71 | 0,59 | 0,45 | 0,55 | 0,52 |
| K | 0,01 | 0,03 | 0,02 | 0,00 | 0,01 | 0,00 | 0,02 | 0,02 | 0,08 | 0,08 | 0,02 | 0,02 | 0,03 | 0,02 |
| An | 81,69 | 48,93 | 63,46 | 93,06 | 87,40 | 88,73 | 60,12 | 58,37 | 19,18 | 22,23 | 46,60 | 55,18 | 44,21 | 50,69 |
| Ab | 17,48 | 48,16 | 34,67 | 6,94 | 11,16 | 10,84 | 38,08 | 39,49 | 73,90 | 69,68 | 51,52 | 43,05 | 52,81 | 47,19 |
| Or | 0,83 | 2,91 | 1,88 | 0,00 | 1,44 | 0,43 | 1,79 | 2,14 | 6,92 | 8,09 | 1,88 | 1,78 | 2,98 | 2,12 |

BA - basaltic andesite; PXT - transitional zone of the clinopyroxenite; Plt - plagioclase; Pl - plagioclase; CPx - clinopyroxene

5. Discussion and conclusions

The petrographic and geochemical characteristics of the subvolcanic basaltic andesites testify that this subvolcanic calc-alkaline to high-K calc-alkaline magmatism is post-collisional, as postulated earlier (Ivanov, 1988; Nedialkov and Pe-Piper, 1998). The studied basaltic andesites are close to the parental magmas for the volcanic series in the Paleogene volcanism in the Eastern Rhodopes. The chondrite normalized REE patterns suggests a weak fractionation of clinopyroxene and plagioclase. The Ta, Nb, P and Ti negative anomalies in spidergrams (Fig. 6) are most likely inherited from the mantle-derived basic magmas that have heated the lower parts of the earth crust in the region. The contents of Ta and Nb are higher than typical subduction-related magmas and the mantle-derived magmas are thought to be generated in enriched mantle after the slab break-off (Yanev, 2003). Investigations of the volcanism in the Eastern Rhodopes (Marchev et al., 1989; 1994; 1998), based on Sr isotope characteristics ($^{87}\text{Sr}/^{86}\text{Sr} = 0.7057 - 0.7083$), have pointed out the important role of the crustal contamination. The raised REE content ascribing amphibolites fusion origin of the melts (Fig. 8), could be interpreted as a geochemical crustal contribution. The crustal contribution most probably occurred during the partial melting of rocks from the lower crust (crust – mantle transition) confirmed by the melting observations on granulites and cumulative pyroxenites.

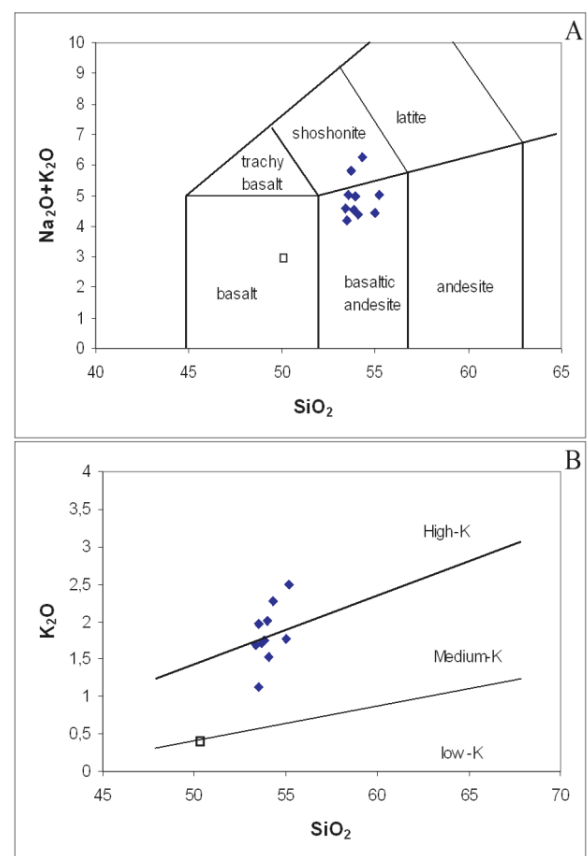


Fig. 5. Systematic of the volcanic rocks after Le Maitre et al.(1989). A – TAS classification diagram. B – Distinction of the volcanic rocks on their potassiac alkalinity using the K₂O – SiO₂ diagram. Symbols as in fig. 4.

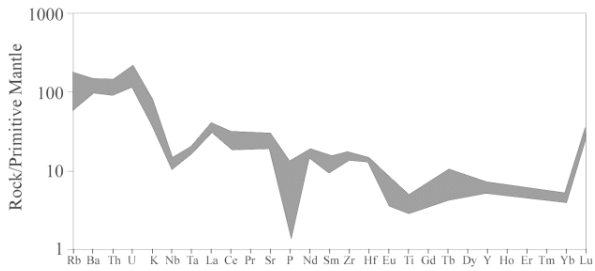


Fig. 6. Primitive mantle normalized spidergram for the trace elements in the basaltic andesites. The normalization values are after Sun and McDonough (1989).

The established xenoliths of granulite and pyroxenite exhibit signs of reworking (component exchange with the magma and beginning of fusion) probably provoked by the relatively more extended in time interaction with the hot basaltic to basaltic andesite magma. In pyroxenites, this is marked by the appearance of the plagioclase inclusions in clinopyroxenes, the small individual plagioclase grains and the miaroles in the transitional zone of influence. The plagioclase nuclei are probably the result of intrapyroxene diffusion of the mineral forming oxides (SiO_2 , Al_2O_3 , CaO). The individual plagioclase grains in the transition zone obviously result from an intergranular fluid-assisted diffusion of components between the clinopyroxenite and the magma attended with decay and shrinkage of the pyroxene grains. The resorption of the pyroxene grains and the magmatic fluids involved lead to the formation at shallower depth of the small miaroles into the transitional zone of the pyroxenite xenolith. Nucleation of plagioclase in pyroxenes and its formation in the transitional zone of the clinopyroxenite presume a relatively poor in H_2O primitive mantle derived magma. At high temperatures ($>1100^\circ\text{C}$) and water content higher than 3 wt %, plagioclase crystallization is suppressed (Müntener et al., 2001; Pichavant and McDonald, 2007). The anhydrous mineral association of the granulite is disequilibrated during the interaction with the hot, fluid-containing magma. The mineral-melt inclusions in plagioclases (relatively rich in Ab component, An_{44-55}) are probably the result of the hosting magma influence.

The plagioclase do not show any sign of melting or subsequent transformation and probably these rocks have been grabbed in relatively shallower depth during the magma ascent. The genesis of these plagioclases has not been determined yet.

Basaltic andesite magma could be primary, formed at the Moho level, as deduced by Mercer and Johnston (2008) for the North Sister volcano. The

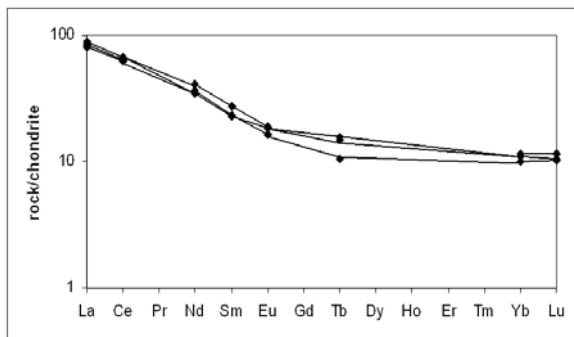


Fig. 7. Chondrite-normalized REE patterns of the sub-volcanic basaltic andesites. The normalizing values are after Boynton (1983).

presence of more primitive volcanic and subvolcanic rocks (basalts, absarokites, basanites, lamprophyres) established in the Eastern Rhodopes (Yanev et al., 1989; Marchev et al., 2006) suggests as a more probable case-scenario the formation of mantle-derived magma that has undergone important evolution and transformation at the crust – upper mantle boundary. The established deep xenoliths give information about the diversity of rocks forming the lithospheric mantle – lower crust transition.

The ascent and the cooling of the magma were probably rapid – a deduction based on the relative preservation of xenoliths (especially plagioclase), the melt inclusions in plagioclases from the granulite and the hyaline texture of the basaltic andesite groundmass.

The formation of saponite in basaltic andesites and granulites postdate the intrusion of the magma in the water rich host rocks at temperatures lower than 110°C , as established by Shau and Peacor (1992) for pillow basalts from DSDP Hole 504B.

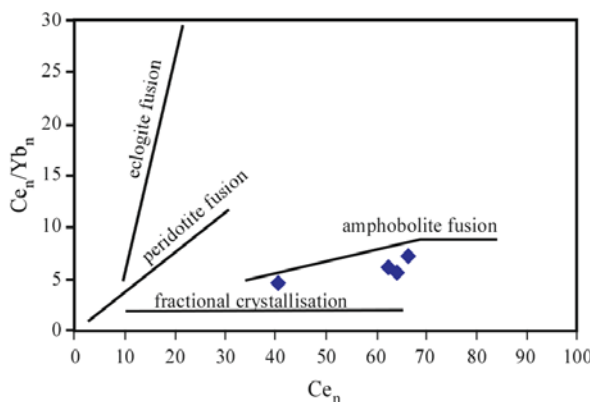


Fig. 8. Ce_n/Yb_n – Ce_n diagram (after Gill 1981) showing changes of Ce and Yb contents due to different type of melting.

Table 3. Major (in wt %) and trace element composition (in ppm) of the subvolcanic basaltic andesites and the granulite xenolith.

| sample № rock | 1216 BA | 4000 BA | 3185 BA | 7 BA | 3195 BA | 3194 BA | 2Kg BA | 4K BA | 1216 xe Granulite |
|--------------------------------|------------|------------|------------|---------|------------|------------|-----------|----------|----------------------|
| SiO ₂ | 51.53 | 52.99 | 51.31 | 52.18 | 52.44 | 52.95 | 51.7 | 51.58 | 47.43 |
| TiO ₂ | 1.06 | 0.66 | 0.92 | 0.93 | 0.7 | 0.67 | 0.63 | 0.7 | 0.72 |
| Al ₂ O ₃ | 13.36 | 16.21 | 16.6 | 17.17 | 16.37 | 16.99 | 16.56 | 18.15 | 16.1 |
| Fe ₂ O ₃ | 5.7 | 5.13 | 4.4 | 4.03 | 5.99 | 5.95 | 6.23 | 5.8 | 7.1 |
| FeO | 3.85 | 3.27 | 3.58 | 3.63 | 2.88 | 1.89 | 2.51 | 2.46 | 2.77 |
| MnO | 0.05 | 0.02 | 0.12 | 0.14 | 0.12 | 0.01 | 0.15 | 0.18 | 0.11 |
| MgO | 5.37 | 5.7 | 4.6 | 5.22 | 5.12 | 4.78 | 5.62 | 4.92 | 7.15 |
| CaO | 7.77 | 8.84 | 8.61 | 9.03 | 7.35 | 7.75 | 8.15 | 8.5 | 10.1 |
| Na ₂ O | 3.77 | 4.04 | 2.83 | 2.96 | 2.56 | 2.42 | 2.67 | 2.96 | 2.56 |
| K ₂ O | 2.16 | 1.68 | 1.92 | 1.92 | 1.68 | 2.4 | 1.68 | 1.08 | 0.36 |
| P ₂ O ₅ | 0.27 | 0.12 | 0.21 | 0.28 | 0.13 | 0.12 | 0.08 | 0.1 | - |
| H ₂ O- | 1.32 | 1.06 | 4.32 | 0.56 | 2.31 | 2.23 | 2.16 | 1.67 | 2.99 |
| LOI | 1.34 | 0.43 | 0.93 | 1.51 | 1.99 | 1.4 | 1.51 | 1.61 | 2.16 |
| Total | 100.61 | 100.16 | 100.35 | 99.58 | 99.96 | 99.64 | 99.65 | 99.71 | 99.55 |
| Norm(Q) | 2.22 | 0.37 | 5.15 | 3.69 | 9.70 | 8.29 | 6.64 | 6.79 | 2.91 |
| Mg# | 65.10 | 69.67 | 64.21 | 67.23 | 68.34 | 72.52 | 71.92 | 69.97 | 74.48 |
| Cr | 49 | 122 | 49 | 53 | 50 | 58 | 55 | 34 | 460 |
| V | 216 | 218 | 200 | 224 | 210 | 219 | 225 | 226 | |
| Ni | 22 | 40 | 23 | 26 | 20 | 25 | 26 | 15 | 96 |
| Co | 32 | | | 26 | | | | | 33 |
| Cu | 37 | 73 | 42 | 26 | 72 | 93 | 40 | 47 | 19 |
| Zn | 83 | 81 | 70 | 76 | 77 | 76 | 71 | 68 | 353 |
| Pb | 28 | 38 | 10 | 21 | 36 | 34 | 33 | 26 | |
| Ga | 19 | 19 | 12 | 15 | 19 | 17 | 17 | 19 | |
| Li | 6 | 8 | 5 | 8 | 6 | 5 | 5 | 4 | 4 |
| Rb | 44 | 70 | 54 | 63 | 91 | 113 | 63 | 39 | 10 |
| Sr | 521 | 473 | 464 | 490 | 420 | 405 | 491 | 619 | |
| Ba | 820 | 951 | 731 | 781 | 877 | 988 | 746 | 879 | 122 |
| Zr | 171 | 161 | 158 | 157 | 187 | 183 | 151 | 161 | |
| Y | 27 | 27 | 27 | 30 | 24 | 28 | 27 | 28 | |
| Nb | 9 | 9 | 8 | 9 | 9 | 10 | 9 | 9 | |
| Ta | 0.77 | | | | | | | | |
| Hf | 4.25 | | | | | | | | |
| Sc | 24.89 | | | | | | | | |
| U | 3.38 | | 2,7 | 2,8 | | | | | |
| Th | 11.06 | 10 | 9.2 | 8.3 | 11 | 12 | 10 | 10 | |
| La | 26.43 | | 27.5 | 24.9 | | | | | |
| Ce | 52.01 | | 54 | 51 | | | | | |
| Nd | 24.48 | | 22 | 21 | | | | | |
| Sm | 5.36 | | 4.51 | 4.45 | | | | | |
| Eu | 1.37 | | 1.2 | 1.34 | | | | | |
| Tb | 0.74 | | 0.5 | 0.7 | | | | | |
| Yb | 2.39 | | 2.07 | 2.27 | | | | | |
| Lu | 0.37 | | 0.33 | 0.34 | | | | | |
| La/Yb | 7.48 | | 8.96 | 7.37 | | | | | |
| Eu/Eu* | 0.83 | | 0.91 | 0.93 | | | | | |

BA - basaltic andesite

Acknowledgements

The author is grateful to Prof. G. Pe-Piper and Prof. A. Harkovska for the analytical results and the initiation of the investigation obtained during previous common works. I also would like to thank Assoc. Prof. Z. Cherneva for many fruitful discussions during the investigation and to the anonymous reviewer for the remarks and suggestions that helped me improve the manuscript. The work is

partly supported by the project 157/009 of the scientific fund of the Sofia University "St. Kliment Ohridski".

References

- Boynton W., 1984. Cosmochemistry of the rare earth elements: Meteorite study. In: Rare Earth Element Geochemistry, Henderson P., (Editor) p. 63-114, Elsevier, Amsterdam.
- Gill J., 1981. Orogenic andesites and plate tectonics.

- Springer Verlag, Berlin, 392p.
- Harkovska A., Yanev Y. and Marchev P., 1989. General features of the Paleogene orogenic magmatism in Bulgaria. *Geologica Balcanica*, 19, 1, 37-72.
- Ivanov R., 1960. Magmatism in the East Rhodope Palaeogene depression. Part I. Geology. *Trudove Geol. Bulg. Ser Geochim Pol. Izkop.*, I, 311-387. (in Bulgarian with German abstract).
- Ivanov Z., 1988. Aperçu général sur l'évolution géologique et structurale du massif des Rhodopes dans le cadre des Balkanides. *Bull. Soc. Geol. Fr.*, 8, IV, 2, 1988, 227-240.
- Le Maitre R., Bateman P., Dudek A., Keller J., Lameyre J., Le Bas M., Sabine P., Schmid R., Sorensen H., Strekeizen A., Woolley A. and Zanettin B., 1989. A classification of igneous rocks and glossary of terms. Recommendations of the international union of geological sciences subcommissionon the systematics of igneous rocks. R. Le Maitre (Ed.), Blackwell, 193p.
- Lilov P., Yanev Y. and Marchev P., 1987. K/Ar dating of the Eastern Rhodopes Paleogene magmatism. *Geologica Balcanica*, 17, 4, 49-58.
- Marchev P., Lilov P., Amov B., Arnaudov V. and Yordanov Y., 1989. Major, trace elements, and isotopic (Sr, Pb) zonation in the Eocene-Oligocene Rhodope Magmatic zone: evidence for subduction processes and crustal influence. XIV congress of CBGA, Sofia, Extended abstracts, 226-229.
- Marchev P., Larson P., Rogers G., Vaselli O. and Raicheva R., 1994. Crustal thickness (CT) control on the Sr, Nd, and O isotopic variation in Macedonean-Rhodope-North Aegean magmatic belt. International Volcanological Congress, IAVCEI, Ankara 1994, Abstracts, p. 6.
- Marchev P., Rogers G., Conrey R., Quick G., Vaselli O. and Raicheva R., 1998. Palaeogene orogenic and alkaline basic magma in the Rhodope zone: relationships, nature of magma source, and role of crustal contamination. In: Tertiary magmatism of the Rhodopean region. *Acta Volcanologica*, 10, 2, 217-232.
- Marchev P., Arai S. and Vaselli O., 2006. 2: Cumulate xenoliths in Oligocene alkaline basaltic and lamprophyric dikes from the eastern Rhodopes, Bulgaria: Evidence for the existence of layered pluton under the metamorphic core complexes. Geological Society of America, Special Paper, 409, 237-258.
- Mercer C. and Johnston A., 2008. Experimental studies of the P-T-H₂O near-liquidus phase relations of basaltic andesite from North Sister Volcano, High Oregon Cascades: constraints on lower-crustal mineral assemblages. *Contributions to Mineralogy and Petrology*, 155, 571-592.
- Fettes D. and Desmons J. (Eds), 2007. Metamorphic rocks: a classification and glossary of terms. Cambridge UP, 244p.
- Moskovski S., Nedyalkov R. and Harkovska A., 1996. Palaeogene subvolcanic basic rocks in Momchilgrad-Arda volcanic region (Eastern Rhodopes). *Compte rendu de l'Academie bulgare des sciences*, 49, 1, 65-68.
- Müntener O., Kelemen P. and Grove T., 2001. The role of H₂O during crystallization of primitive arc magmas under uppermost mantle conditions and genesis of igneous pyroxenites: an experimental study. *Contribution to Mineralogy and Petrology*, 141, 643-658.
- Nedialkov R. and Pe-Piper G., 1998. Petrology of the volcanism in the southern part of the Momchilgrad-Arda volcanic region, southern Bulgaria. *Acta Volcanica*, 10, 2, 243-253.
- Nimis P., 1999. Clinopyroxene geobarometry of magmatic rocks. Part 2. Structural geobarometers for basic and to acid, tholeiitic and mildly alkaline magmatic systems. *Contribution to Mineralogy and Petrology*, 135, 62-74.
- Pichavant M. and Macdonald R., 2007. Crystallization of primitive basaltic magmas at crustal pressures and genesis of the calc-alkaline igneous suite: experimental evidence from St Vincent, Lesser Antilles arc. *Contribution to Mineralogy and Petrology*, 154, 535-558.
- Putirka, K., 2008. Thermometers and Barometers for Volcanic Systems. In: Putirka, K., Tepley, F. (Eds.), Minerals, Inclusions and Volcanic Processes, *Reviews in Mineralogy and Geochemistry*, Mineralogical Soc. Am., v. 69, pp. 61-120.
- Shau Y.-H. and Peacor D., 1992. Phyllosilicates in hydrothermally altered basalts from DSDP Hole 504B, Leg 83 – a TEM and AEM study. *Contributions to Mineralogy and Petrology*, 112, 119-133.
- Sun S. and McDonough W., 1989. Chemical and isotopic systematics of ocean basalts: implications for mantle composition and processes. In: Saunders A., Norry M (Editors), *Magmatism in the Ocean Basins*, p. 313-345, Geological Society Special Publication.
- Velchev Tz., Dimitrov R. and Mavroudchiev B., 1971. About the deep structure of the East Rhodopean block and the central Rhodopean deep fault zone. *Compte rendus de l'academie bulgare des sciences*, 24, 9, 1231-1234. (in Russian).
- Weels P. R. A., 1977. Pyroxene thermometry in simple and complex systems. - *Contr. Mineral. Petrol.*, 62, 129-139.
- Yanev Y., 2003. Mantle source of the Paleogene collision-related magma of the Eastern Rhodopes (Bulgaria) and Western Thrace (Greece): Characteristics of the mafic magmatic rocks. *N. Jb. Miner. Abh.*, 178, 2, 131-151.
- Yanev Y., Mavroudchiev B. and Nedyalkov R., 1989. Paleogene collision-related basalts and basaltic andesites in the Eastern Rhodopes, Bulgaria. *Journal of volcanology and geothermal research*, 37, 187-202.
- Yossifov D. and Pčelarov V., 1977. A scheme of the thickness of the Earth's Crust in the Balkan Peninsula and some features of its structure. *Geologica Balcanica*, 7, 2, 7-22. (In Russian with English abstract).